Zagazig University Medical Journal
www.zumj.journals.ekb.eg
https://dx.doi.org/10.21608/zumj.2022.126519.2498 Volume 28, Issue 4, July 2022(848-855)
Manuscript ID ZUMJ-2203-2498 (R1)
DOI **10.21608/zumj.2022.126519.2498**

ORGINAL ARTICLE

Feasibility of Apparent Diffusion Coefficient Value in Predicting Nature of Skull Base Lesions

Marwa Elsayed Abd Elhamed[1*], Manar Awad Bessar[1], Mohamed Ismail Ahmed Hammad[2], Nader Ali Alayouty[1]
[1]Radiodiagnosis Department, Faculty of Medicine, Zagazig University, Zagazig, Egypt
[2]Radiodiagnosis Department, Faculty of Medicine, El Azhar University, Egypt

[1, *]Corresponding author:
Marwa Elsayed Abd Elhamed Saleh
E-mail: dr.meroelsayed34@gmail,.com
[1]Radiodiagnosis Department, Faculty of Medicine, Zagazig University, Zagazig, Egypt

ABSTRACT

Background: The base of the skull is a relatively common site for neoplasms and their imaging features can overlap. The correct diagnosis decision has sometimes been hardly made by routine magnetic resonance imaging (MRI) which can always be insufficient. The primary purpose of this study was to evaluate the feasibility of apparent diffusion coefficient (ADC) value measurement in distinguishing skull base lesions

Methods: Between April 2020 and June 2021, a prospective study was conducted at the Department of Radiodiagnosis, University Hospitals of Zagazig, involving 45 patients clinically suspected of having skull base neoplasms diagnosed by CT. Our results were linked to histopathologic findings in all patients

Results: Our study included 23 benign neoplastic lesions and 22 malignant neoplastic lesions, the highest mean ADC value for malignant tumors was 1.15± 0.22 x 10^{-3} mm^2/s, while the highest ADC value for benign tumors was 1.71 x 10^{-3} mm^2/s, It was found that a cut off value of 1.2 x 10^{-3} mm^2/s between benign and malignant lesions with an accuracy of 95.56%, a sensitivity of 90.91%, a specificity of 100%, a positive predictive value (PPV) of 100%, and a negative predictive value (NPV) of 92% at an AUC of 0.901

Conclusions: The Diffusion Weighted Imaging (DWI) and ADC value are non-invasive, quantitative methods for detecting nature of the skull base neoplasms.

Keywords: Skull Base Mass Lesions; Conventional MRI; Diffusion Weighted Imaging; Apparent Diffusion Coefficient Value

INTRODUCTION

The anatomical area of the skull base is challenging to diagnose and treat using imaging. Although it's a common site for neoplasms, it's difficult to reach because it's confined between the contents of the skull, face, and neck. Because brain structures and arteries are densely packed and cross many layers of tissues, there is a limited tolerance for manipulation [1].

On standard magnetic resonance imaging (MRI), non-contrast T1W-weighted images (T1W), T2W-weighted images (T2W), and post-contrast T1W-weighted images are used to diagnose skull base brain cancers [2]. Traditional MRI scans can reveal structural informations including tumor size, location, and morphology, but not tumor grade, aggressiveness, or histological criteria. Diffusion-weighted imaging (DWI) and other imaging modalities have recently been identified as useful for this purpose [3].

Water flow in intracellular, extracellular, and transcellular domains is detected using diffusion-weighted imaging (DWI), a multi-section spin-echo planar imaging (EPI) technique. This is useful for distinguishing benign (low-grade) from malignant (high-grade) brain cell tumors [4]

This dissertation's main goal is to aid in radiological differential diagnosis. The imaging characteristics of benign and malignant skull base lesions are quite similar, and they are frequently seen together. As a result, the goal of our research was to see how efficient the DWI and ADC values were at distinguishing between different skull base brain tumors, as well as how these results correlated with histological analyses.

PATIENTS AND METHODS

From April 2020 to June 2021, 45 patients were enrolled in prospective research at Zagazig University Hospitals' Department of Radiodiagnosis (28 males and 17 females; average age 47.6 years). Neurosurgery, ENT departments, and outpatient clinics were among the sources of referrals.

Clinically suspected and CT-diagnosed skull base neoplasms were the inclusion criteria.

Individuals with MRI contraindications, those having chemotherapy or radiation therapy, cases with a known history of operated brain neoplasms were all ruled out.

All subjects provided written informed consent, and the study was approved by the research ethical committee of Zagazig University's Faculty of Medicine. The research was conducted out in conformity with the World Medical Association's Code of Ethics (Declaration of Helsinki) for human studies.

All included study patients underwent clinical history taking, contrast enhanced MRI, DWI and ADC value measurement, then the ADC values were correlated to the histopathological findings of 27 surgically removed lesions and 18 tissue biopsied lesions.

Scanning Protocol

Conventional Magnetic Resonance Imaging (MRI)

All MRIs were done in the supine position using a Philips Achieva class IIa MR machine (1.5 T) with a standard head surface coil. All patients were instructed to remove all metal objects from their possessions and were advised of the duration and significance of their immobility. Prior to the administration of contrast, a scout sagittal T1-weighted view was taken to confirm the patient's precise position and to serve as a localizer for subsequent slices. Multiple pulse sequences were then used to obtain axial images, followed by coronal and/or sagittal images, depending on the location of the pathology encountered. For midline lesions, sagittal planes were used, while coronal images were more useful for lateral lesions.

The contrast medium was Magnevist [gadolinium di-ethylene tri-amine penta-acetic acid (Gd-DTPA)] which was given intravenously at a dose of 0.1 mmol/kg body weight. T1-WIs were taken right after the contrast injection was finished.

The following protocol was used to examine all cases:

T1-WI in the sagittal plane as a localizer:

Axial and coronal spin-echo sequences, short Repetition Time/Echo time (TR/TE) [T1-weighted images; TE = 10–12 m/s, TR = 400–600 m/s]

Axial rapid spin-echo sequences, long TR/TE (T2-weighted images): TE = 70–90 m/s TR = 2800–3500 m/s

Short TR/TE (T1-weighted pictures) post-contrast axial, sagittal, and coronal spin-echo sequences: TR = 400–600 m/s TE = 10–12 m/s

In axial images, the Field of View (FOV) was 24–18 cm, while in coronal images, the FOV was 30–22 cm.

Matrix (frequency × phase) 192 × 160., 6 mm thick slices with a 2 mm spacing (In all sequences)

Diffusion Weighted Imaging (DWI) and (ADC) value

The DWI imaging sequence was a multi-section single-shot spin-echo EPI sequence (TR/TE/number of excitations: 4200/140 ms/I) with diffusion sensitivities of 0, 500, and 1000 s/mm^2 and TR/TE/ number of excitations: 4200/140 ms/I. Diffusion gradients were applied in three orthogonal directions at a time (X, Y and Z directions). All images were created using slices with a thickness of 5 mm, a spacing between slices of 1 mm, a FOV of 240 mm, and a matrix of 128 X 256. The acquisition took 80 seconds in total. Orthogonal pictures, trace images, and ADC maps were all acquired. The ADC maps were computed and incorporated in the sequence automatically by the MRI software. ADC measurements were taken in several regions of interest (ROI) of the lesions, with the cystic sections of the lesions being avoided as much as feasible, as this could result in erroneously high ADC values. The ADC readings were given in mm^2/s. A histological investigation was done in each patient to determine the final diagnosis.

Statistical Analysis:

The data was computerized and statistically analyzed using the SPSS (Statistical Package for Social Science) application version 18.0. To present qualitative data, we employed frequencies and relative percentages. To report quantitative data, the mean and standard deviation (SD) were utilized (standard deviation) for normally distributed data. Receiver Operating Characteristics (ROC) curves with high accuracy and sensitivity were used to calculate the cutoff value. Reliability was evaluated through sensitivity, specificity, positive predicted value, negative predicted value and accuracy. Non-significant results were indicated by a P-value > 0.05, significant results were indicated by a P-value < 0.05, and highly significant results were indicated by a P value of 0.01 or less. The data was examined to see if any statistically significant differences existed.

RESULTS

All patients in our study ranged from 32 to 65 years old, with an average age of 47.6 years. The majority of patients (28 cases; 62.2 %) were men, while the rest were women (17 cases; 37.8 %). Headaches were the most prevalent complaint in 38 cases (84.4%), vomiting in 24 cases (53.3%), dizziness in 15 cases (33.3%), and epistaxis in four cases (8.9 %). Patients were grouped into three categories based on the location of the lesion: anterior, middle, and posterior cranial fossa lesions

comprising 8 (17.8%), 28 (62.2%), and 9 (20%) cases, respectively. According to the histological findings, study cases were divided into 23 (51.1%) benign and 22 (48.9%) malignant neoplasms: the benign neoplasms included meningioma 12 (26.7%), pituitary macroadenoma 5 (11.1%) and schwannoma 6 (13.3%) while the malignant neoplasms included chordoma 7 (15.6%), sinonasal squamous cell carcinoma (SCC) 11 (24.4%) and adenoid cystic carcinoma 4(8.9%). Based on imaging specific signs, we observed dural tail sign at 12 cases (26.7%), bone invasion 18 cases (40%), and hyperostosis 8 cases (17.8%) (**Table 1)**.

Hyperintensity, isointensity, and hypointensity were elicited in 28 lesions (62.2 %), 13 lesions (28.9 %), and 4 lesions (8.9%) of the T2-weighted images, respectively. 20 lesions (44.4%) of the diffusion-weighted images have diffusion hyperintensity, while 7 lesions (15.6%) are isointense, and 18 lesions (40%) are hypointense. When the DWI features of skull base tumors were taken into account, restricted diffusion was found in 20 lesions (44.4%) which were found to be of malignant nature (**Table 2)**.

ADC value was in the range of (1.4 to 1.97 x 10^{-3} mm^2/s) among benign neoplasms, with the highest mean ADC value in pituitary macroadenoma (1.71 ± 0.15 x 10^{-3} mm^2/s). ADC ranged from 0.5 to 1.750 x 10^{-3} mm^2/s among malignant lesions (p=0.004) but one of the limitations is that the highest mean ADC value in both adenoid cystic carcinoma and chordoma were (1.12 ± 0.19 x 10^{-3} mm^2/s) and (1.15 ± 0.22 x 10^{-3} mm^2/s) that were wrongly misinterpreted as a benign tumor (**Table 3)**.

We found out that ADC value measurement can correctly diagnose 23 of 23 actual benign lesions and 20 of 22 true malignant lesions compared to the gold standard of histopathological evaluation. The two false negative cases were finally diagnosed as adenoid cystic adenocarcinoma and chordoma (**Table 4).**

At an AUC of 0.901, an ADC cut off value of 1.2 x 10^{-3} mm^2/s was used to distinguish between benign and malignant skull base lesions. We reported accuracy of 95.56 %, sensitivity of 90.91 %, specificity of 100%, positive predictive value (PPV) of 100 % and a negative predictive value (NPV) of 92 % **(Table 5) and [Figure 1]. Figures (2), (3) and (4)** show demonstrative cases.

Table (1): Demographic Characteristics of study of 45 patients

Factor	Category	Patient no.	Percent
Age	32-45	19	42.2%
	46-65	26	57.8%
Sex	Male	28	62.2%
	Female	17	37.8%
Presenting symptoms	Headache	38	84.4%
	Vomiting	24	53.3%
	Dizziness	15	33.3%
	Epistaxis	4	8.9%
Site	Anterior cranial fossa	8	17.8%
	Middle cranial fossa	28	62.2%
	Posterior cranial fossa	9	20%
Histopathology	Meningioma	12	26.7%
Benign n.=23(51.1%)	macroadenoma	5	11.1%
	Schwannoma	6	13.3%
	Chordoma	7	15.6%
Malignant n.=22(48.9%)	Sino nasal SCC	11	24.4%
	Adenoid cystic Ca.	4	8.9%
Specific signs	Dural tail	12	26.7%
	Bone invasion	18	40%
	Hyperostosis	8	17.8%

Table (2): Study pathological entities based on T2WI, DWI & ADC.

Lesions	T2WI no. (%)	DWI no. (%)	ADC no. (%)
Benign (n=23)			
Meningioma (n=12)	*** 7(15.6%) ** 5(11.1%)	* 9 (20%) ** 3 (6.7%)	* * 12 (26.7%)
Macroadenoma (n=5)	*** 4 (8.9%) ** 1(2.2%)	* 5 (11.1%)	** 1(2.2%) *** 4(8.9%)
Schwannoma (n=6)	*** 4(8.9%) ** 2 (4.4%)	** 2 (4.4%) * 4 (8.9%)	* * 2 (4.4%) *** 4 (8.9%)
Malignant (n=22)			
Chordoma (n=7)	*** 7 (15.6%)	*** 7(15.6%)	* 7(15.6%)
Sino nasal SCC (n=11)	*** 6 (13.3%) ** 5 (11.1%)	*** 10(22.2%) *** 1(2.2%)	* 10(22.2%) *** 1(2.2%)
Adenoid cystic Ca. (n=4)	* 4(8.9%)	*** 3(6.7%) ** 1(2.2%)	* 4(8.9%)

*Hypointense, **isointense & ***hyperintense.

Table (3): Study pathological entities based on mean ADC value

	ADC. (X10^{-3}mm^2/s) Min.-max.	(Mean ±SD.)	Median	P value
Meningioma (n=12)	1.54 -1.815	1.6 ± 0.24	1.4	
Pituitary macroadenoma (n=5)	1.64 – 1.97	1.71 ± 0.15	1.33	
Acoustic Schwannoma (n=6)	1.4- 1.73	1.16± 0.12	1.23	
Clival chordoma (n=7)	0.5 -1.750	1.15±0.22	0.8	0.004
Sino nasal SCC (n=11)	0.70-1.10	0.89 ± 0.16	0.65	
Adenoid cystic Ca. (n=4)	0.80-1.69	1.12± 0.19	1.10	

Table (4): Agreement between ADC value & histo-pathological outcomes

Diagnosis	Histopathology				Sensitivity	Specificity	PPV	NPP	Accuracy
ADC value	Benign (n=23)		Malignant (n=22)		90.91	100	100	92	95.56
	No.	%	No.	%					
Benign	23	51.1	2	4.4					
Malignant	0	0.0	20	44.4					

Table (5): ADC value validity

	Senstivity%	Specifity%	PPV%	NPV%	ACU%	AUC%	Cut off v.
ADC	90.91	100	100	92	95.56	0.901	1.2

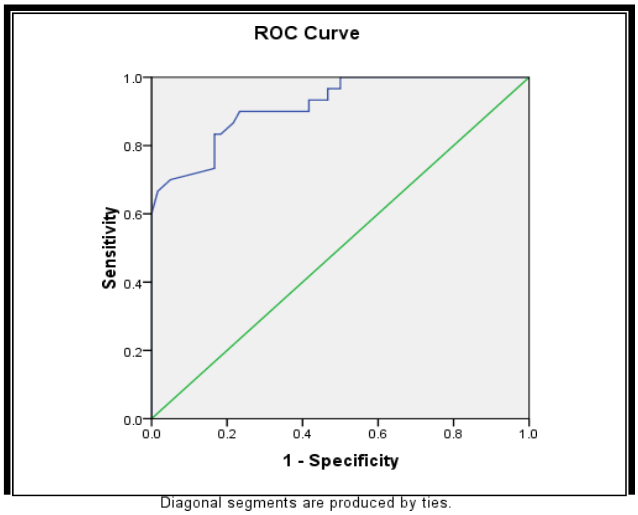

Figure (1): Receiver Operating Characteristic (ROC) curve. An apparent cutoff diffusion coefficient (ADC) value of 1.2 x 10^{-3} mm^2/s with an area under the curve (AUC) of 0.901 was used to discriminate between malignant and benign tumors.

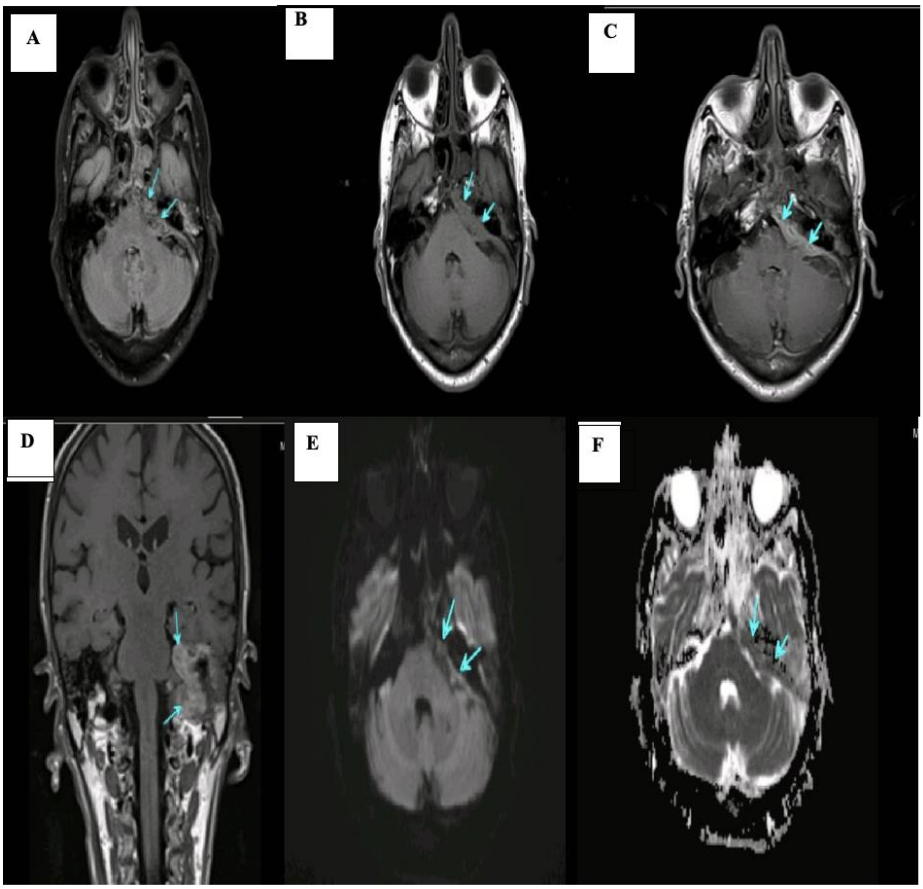

Figure (2): MRI findings in 48-year-old female patient presented with dizziness and headache. (A) axial T1W and (B) axial T2W show extra-axial left sided CPA tentorial isointense sheet-like lesion (arrows)(C) and (D) contrast enhanced axial and coronal cuts show post-contrast heterogenous enhancement (arrows), (E) and (F) DWI and ADC map images show relative restricted diffusion (arrows) and high ADC value (1.69 x 10^{-3} mm2/S), pathologically proved adenoid cystic carcinoma.

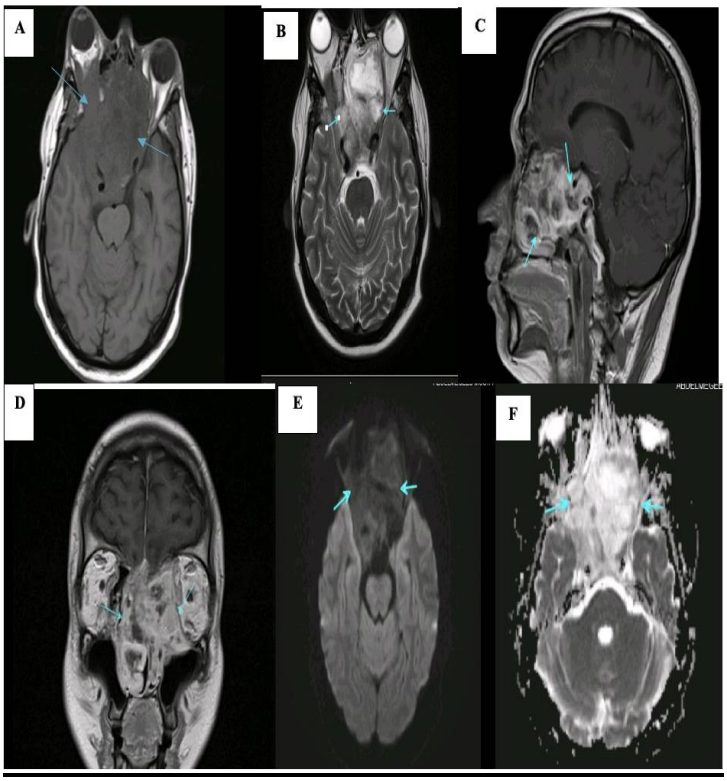

Figure (3): MRI findings in male patient aged 37 years presented with epistaxis and headache. (A) Axial cut T1W and (B) T2W show abnormal signal intensity large destructive lesion infiltrating the front-ethmoidal and sphenoidal sinuses with Rt orbital and nasal extension (arrows) (C) and (D) Contrast- enhanced sagittal and coronal cuts display moderate heterogeneous enhancement(arrows) (E) and (F) DWI and ADC map images show scanty areas of restricted diffusion (arrows) and low ADC value (0.73 x 10^{-3} mm2 /S), pathologically proved Sino nasal SCC.

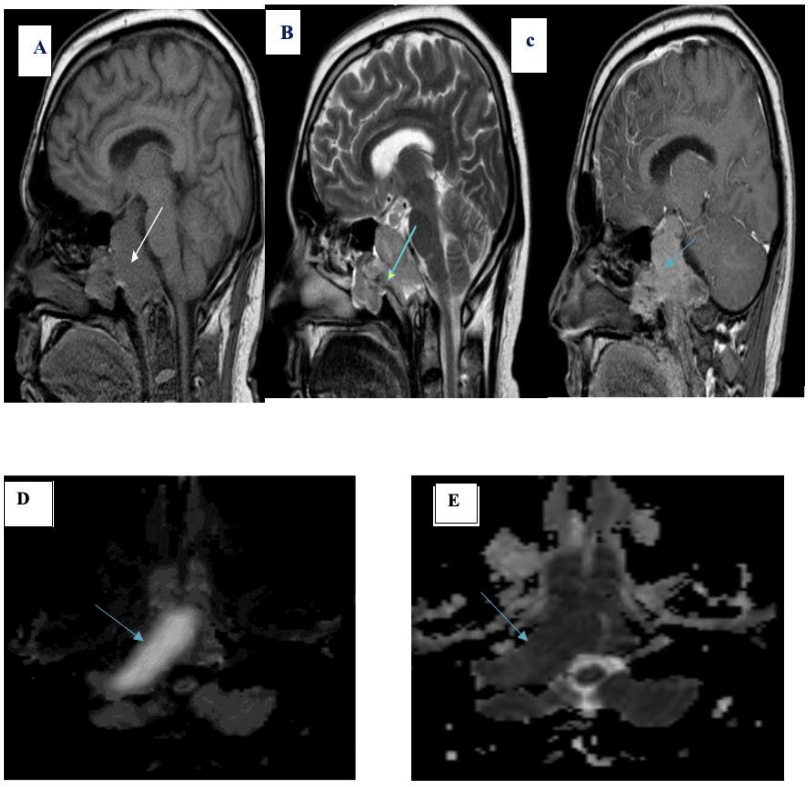

Figure (4):MRI findings in male patient aged 56 presented with vomiting and headache, (A) and (B) Sagittal T1W and T2W cuts show large isointense soft tissue lesion infiltrating the clivus with invading sphenoid sinus, nasopharynx cavity and Rt cerebellopontine angle region (arrows), (C) contrast-enhanced sagittal cut shows mild homogenous enhancement (D) and (E) DWI and ADC map images show restricted diffusion and a high ADC -value (1.75 x 10^{-3} mm2 /S), pathologically proved clivus chordoma

DISCUSSION

Because skull base is difficult to be assessed clinically, imaging is essential for detecting abnormalities [5-6]. Although conventional MRI is insufficient for diagnostic purposes, it is used to analyze the location, size, morphology, and connection of mass skull base lesions to key structures. Additional imaging modalities as DWI are necessary to identify and distinguish skull base mass lesions [4].

DWI can give critical information regarding a tumor's cellularity and water mobility, as well as the water content of its surrounding matrix. It can also be used to classify lesions at the skull base into low, middle, and high cellularity, making them easier to identify, define, and discriminate [7].

In this investigation, 45 patients with clinically suspected and CT-diagnosed skull base neoplasms received conventional MRI and DWI to see if DWI and ADC values may help identify benign from malignant lesions. In every case, the findings matched the histological findings.

The majority of patients were male 28 cases(62.2 %), while females were17 cases(37.8%). Cases ranged from 32 to 65 years, with an average age of 47.6 years. We diagnosed 23 benign and 22 malignant cases.

Headache and mental abnormalities were the most prevalent symptoms, accounting for 84.4 % of all cases (38 out of 45 cases in our study) in harmony with studies reported by Tsikoudas and Martin's study [8] and Taillibert et al. [9].

According to T2-weighted images, Haque et al. [10] reported that hyperintense lesions were the most common, accounting for 84.6 % (22 of 26 cases in their study); this was consistent with our findings, which revealed hyperintensity, isointensity, and hypointensity in 28 cases (62.2 %), 13 cases (28.9 %), and 4 cases (8.9%), respectively.

Twenty lesions (44.4%) of the diffusion-weighted images had diffusion hyperintensity, while 7 lesions (15.6%) were isointense and 18 lesions (40%) were hypointense, which is in line with Abdel Razek et al's study [11].

Regarding the DWI characteristics of skull base tumors, Thukral et al. [12] reported that all lesions had facilitated diffusion and no lesion was restricted; however, our findings showed that restricted diffusion was observed in 20 lesions, accounting for 44.4%, all cases were malignant in nature, this discrepancy might be owing to the benign nature of thukral et al's cases.

The highest mean ADC value for malignant tumors was 1.15± 0.22 x 10^{-3} mm^2/s, while the highest ADC value for benign tumors was 1.71 x 10^{-3} mm^2/s. There was a statistically significant difference in ADC values between aggressive and benign tumors (p-value = 0.004) which is consistent with the results of Abdel Razek et al. [11] who discovered that the mean ADC value of malignant tumors was 1.0020 x 10^{-3} mm^2/s, while the value of benign tumors was 1.630 x 10^{-3} mm^2/s, with a statistically significant difference in ADC values between benign and malignant lesions. These findings can be explained by differences in histological features between benign and malignant tumors; malignant tumors have larger nuclei, hyperchromatism, and angulation of nuclear contour, among other structural changes; benign tumors have smaller nuclei, hyperchromatism, and angulation of nuclear contour, among other structural changes; and benign tumors have smaller nuclei, hyperchromatism, and angulation of nuclear contour, among other structural changes in ADC values [13-14].

Imaging and histopathologic findings were consistent in 100% of benign cases and 86.9% of malignant cases. One case out of seven clivus chordoma cases was mistaken as a benign tumor due to its high ADC value, which was corroborated by histopathologic findings. This is most probably because the tumor contains more fluid, which promotes diffusion [15]. This corresponds to Yeomet al. [16], who found that the mean ADC value for poorly differentiated chordomas was (0.875 x 10^{-3} mm^2/s) whereas the mean ADC value for typical chordomas was 1.4 x 10^{-3} mm^2/s [15]. The histological findings revealed a high ADC value in one example of four adenoid cystic carcinoma lesions that were misinterpreted as benign tumors. This was clarified according to earlier studies [17]. The high mucus content and cystic components are responsible for the high ADC value

Our findings show that the ADC cut-off value (1.2 x 10^{-3} mm2/s) used to distinguish between benign and malignant skull base lesions has an AUC of 0.901 and an accuracy of 95.56 %, as well as a sensitivity of 90.91%, a specificity of 100 %, a positive predictive value (PPV) of 100 %, and a negative predictive value (NPV) of 92 %, which is consistent with Abdel Razek et al. [11], noting that a cut-off value of 1.3 × 10^{-3} mm2/s has been shown to separate benign from malignant neoplastic lesions, showed high sensitivity (94%), specificity (93%), PPV (93%), NPV (94%) and AUC of (0.923).

Diffusion-weighted imaging and ADC analysis were found to be more sensitive and specific in diagnosing and defining skull base lesions, as well as more effective in evaluating whether or not the lesions were malignant. Our study had various limitations, including a small number of patients,

which hindered statistical analysis in addition to partial volume averaging and susceptibility aberrations of skull base bone lesions which may have influenced the obtained ADC values.

CONCLUSION

DWI and ADC value have showed potential as a non-invasive, quantitative approach to skull base lesions for diagnostic decision making and treatment plan. Therefore, they should be used as a supplement to conventional MRI for describing skull base masses.

CONFLICTS OF INTEREST: None
FINANCIAL DISCLOSUREs: None

REFERENCES

1. Thust S C, Yousry T\: Imaging of skull base tumors, Rep Pract Oncol Radiother; (2016), 21(4): 304-18.
2. Nardone V, Tini P, Biondi M, Sebaste L, Vanzi E, De Otto G, et al.: Prognostic value of MR imaging texture analysis in brain non-small cell lung cancer oligo-metastases undergoing stereotactic irradiation; Cureus;(2016); 25;8(4): e 584-98.
3. Peet A C, Arvanitis T N, Leach M O, Waldman AD.: Functional imaging in adult and paediatric brain tumors. Nat Rev Clin Oncol; 2012: 9(12):700-5.
4. Stadnik TW, Demaerel P, Luypaert RR, Chaskis C, Van Rompaey KL, Michotte A, et al. Imaging tutorial: differential diagnosis of bright lesions on diffusion weighted MR images. Radiographics**.** 2003;23(1):1–7
5. Parmar H, Gujar S, Shah G, Mukherji SK. Imaging of the anterior skull base. Neuroimaging Clin N Am;(2009); 19(3): 427-39.
6. Raut A A, Naphade P S, Chawla A. Imaging of skull base: Pictorial essay. Indian J Radiol Imag 2012; 22: 305–16.
7. Moritani T, Ekholm S, Westesson P-LA. Diffusion-weighted MR imaging of the brain: Springer Science and Business Media; 2009: (1): 1-5
8- Tsikoudas A, Martin Hirsch DP.: Olfactory groove meningiomas. Clin. Otolaryngol.; (2000): 24(6) :507- 9.
9- Laigle-Donadey F, Taillibert S, Martin-Duverneuil N, Hildebrand J, Delattre JY.: Skull-base metastases. Journal of neuro-oncology; (2005):75 (1): 63-9
10- Haque S, Hossain A, Quddus M A, Jahan MU. Role of MRI in the evaluation of acoustic schwannoma and its comparison to histopathological findings. Bangladesh Med. Res. Counc. Bull.; (2011); 37(3): 92-6.
11-Abdel Razek A, Mossad A, Ghonim m.: Role of diffusion-weighted MR imaging in assessing malignant versus benign skull-base lesions, head and neck radiology; (2011), 116:125–32
12- Singh K, Singh M P, Thukral C L, Rao K, Singh K, Singh A, Role of magnetic resonance imaging in evaluation of cerebellopontine angle schwannomas. Indian J Otolaryngol Head Neck Surg; (2015) 67(1) :21-27.
13. Koh D., Collins D.: Diffusion weighted MRI in the body: applications and challenges in oncology. Am J Roentgenol AJR (2007) 188:1622–35.
14. White ML, Zhang Y, Robinson RA: Evaluating tumors and tumorlike lesions of the nasal cavity, the paranasal sinuses, and the adjacent skull base with diffusion-weighted MRI. J Comput Assist Tomogr (2006) 30:490–5.
15. Van Rijswijk CS, Kunz P, Hogendoorn PC, Taminiau AH, Doornbos J, Bloem JL: Diffusion–weighted MRI in the characterization of soft tissue tumors. J Magn Reson Imag (2002) 15: 302-7.
16.Yeom K W, Lober R M, Mobley B C, Harsh G, Vogel H, Allagio R et al., Diffusion weighted MRI: distinction of skull base chordoma from chondrosarcoma. Am. J. Neuroradiol., (2013), 34 (5):1056-61.
17. Yerli H, Agildere A, Aydin E, Geyik E, Haberal N, Kaskati T et al., Value of apparent diffusion coefficient calculation in the differential diagnosis of parotid gland tumors. Acta Radiol; (2007), 48:980–7.

To Cite:
Abd Elhamed, M., Bessar, M., Ahmed Hammad, M., Alayouty, N. Feasibility of Apparent Diffusion Coefficient Value in Predicting Nature of Skull Base Lesions. *Zagazig University Medical Journal*, 2022; 28(4): 848-855. doi: 10.21608/zumj.2022.126519.2498